Ion–ion Proton Transfer Reactions of Bio-ions Involving Noncovalent Interactions: Holomyoglobin

James L. Stephenson, Jr., Gary J. Van Berkel, and Scott A. McLuckey
Chemical and Analytical Sciences Division, Oak Ridge National Laboratory, Oak Ridge, Tennessee, USA

Multiply protonated horse skeletal muscle holomyoglobin and apomyoglobin have been subjected to ion–ion proton transfer reactions with anions derived from perfluoro-1,3-dimethylcyclohexane in a quadrupole ion trap operated with helium as a bath gas at 1 mtorr. Neither the apomyoglobin nor holomyoglobin ions show any sign of fragmentation associated with charge state reduction to the 1+ charge state. This is particularly noteworthy for the holomyoglobin ions, which retain the noncovalently bound heme group. For example, no sign of heme loss is associated with charge state reduction from the 9+ charge state of holomyoglobin to the 1+ charge state despite the eight consecutive highly exothermic proton transfer reactions required to bring about this charge change. This result is consistent with calculations that show the combination of long ion lifetime and the high ion–helium collision rate relative to the ion–ion collision rate makes fragmentation unlikely for high mass ions in the ion trap environment even for noncovalently bound complexes of moderate binding strength. The ion–ion proton transfer rates for holo- and apomyoglobin ions of the same charge state also were observed to be indistinguishable, which supports the expectation that ion–ion proton transfer rates are insensitive to ion structure and are determined primarily by the attractive Coulomb field. (J Am Soc Mass Spectrom 1997, 8, 637–644)

High mass multiply charged ions derived from biomolecules have become commonplace in mass spectrometry, particularly with the advent of electrospray (ES) [1–5], but also with the introduction of matrix assisted laser desorption [6–8] and massive cluster impact [9, 10]. In many respects, the multiple charging phenomenon facilitates mass measurement by, for example, bringing the mass-to-charge ratios of high mass molecules into a range amenable for analysis by a variety of mass analyzers. Multiple charging, on the other hand, can also lead to complications, as in the analysis of mixtures. A number of studies have been reported that describe situations in which the manipulation of ion charge states is desirable. These include, among others, product ion charge state determination [11–13], resolution of mixture components [14, 15], and determination of the charge of a single very high mass ion [16]. The most commonly employed technique involves the reduction of charge of a highly charged ion via proton transfer reactions with neutral molecules [17–29]. In addition to the application of ion–molecule proton transfer reactions for charge state reduction, such chemistry also has been used to probe fundamental aspects of gaseous multiply charged bio-ions [17–29]. Ion–molecule reactions are most effective for highly charged ions, but reaction efficiencies become low as the charge is reduced [17, 20, 21, 23, 25]. For this reason, it has been difficult to produce singly charged ions from high mass multiply charged ions via ion–molecule proton transfer chemistry. The use of ion–ion reactions involving multiply charged ions reacting with singly charged ions of opposite polarity in a Paul trap, on the other hand, has been demonstrated recently to be effective at reducing charge states to arbitrarily low values, at least for proteins [30]. Evidence has been presented that these reactions take place at constant efficiency [30]. Given the high exothermicity associated with ion–ion neutralization reactions, it is likely that the reactions also take place with unit efficiency. Ion–ion proton transfer reactions therefore appear to be more effective at reducing charge states than ion–molecule reactions, particularly at low charge states.

The facility with which highly charged ions can be reduced in charge has been attributed to the high exothermicities of ion–ion reactions and the fact that, unlike ion–molecule proton transfer reactions, there is

Address reprint requests to Dr. Scott A. McLuckey, Oak Ridge National Laboratory, P.O. Box 2008, Oak Ridge, TN 37831-6365. E-mail: mcluckey@ornl.gov

1044-0305/97/$17.00
PII S1044-0305(97)00023-8

Received December 4, 1996
Revised February 5, 1997
Accepted February 6, 1997

no Coulomb barrier in the product ion channel. Reaction exothermicities of ion–ion proton transfer reactions involving a multiply protonated reactant, for example, are determined by the difference between the proton affinity of the anionic reactant and the proton affinity of the cationic product. Anion proton affinities are significantly higher than those of neutral molecules and are expected to be even higher than those of cations [31]. Therefore, ion–ion proton transfer reactions between multiply protonated biomolecules and anions that behave as Brønsted bases are highly exothermic (in general, by at least 4 eV) at all charge states, with the highest exothermicities associated with the highest charge states. It has been shown that highly exothermic *electron* transfer reactions involving multiply charged anions derived from small oligonucleotides (less than seven residues) in reactions with rare gas cations result in extensive fragmentation of the anion product [32]. Recent studies that used less exothermic electron transfer reactions involving multiply charged oligonucleotide anions of similar size showed less fragmentation [33]. These results demonstrate that at least some of the ion–ion reaction exothermicity is partitioned into the bio-ion product and can result in the cleavage of covalent bonds, at least for electron transfer reactions. Provided ion–ion proton transfer reactions proceed through relatively long-lived collision complexes, and there is good evidence to suggest that they do [34], some of the reaction exothermicity also should be partitioned into the cationic product. However, there is very little evidence thus far for fragmentation of the cationic product formed from a more highly charged cation after reaction with an anion.

Despite the relatively high exothermicities of ion–ion proton transfer reactions, the likelihood for fragmentation of high mass ions is minimized by the high numbers of degrees of freedom of bio-ions and the high ion–helium collision rate in the ion trap. The lifetime of an excited ion is, however, highly dependent upon the lowest critical energy for decomposition. Although dissociation of covalently bound polypeptides may not occur as a result of ion–ion proton transfer, it stands to reason that less strongly bound systems may not survive an ion–ion proton transfer reaction of moderate-to-high exothermicity. To investigate this hypothesis, horse skeletal muscle myoglobin was chosen for study because the noncovalently bound holomyoglobin form (heme-containing) has been extensively studied [35–39] and because the loss of the heme group to form apomyoglobin is a relatively facile process. Ion trap collisional activation has shown loss of heme from holomyoglobin ions to occur exclusive of fragmentation at covalent bonds [40]. Furthermore, loss of the heme group from holomyoglobin also can be observed by raising the temperature of the helium bath gas by a few tens of degrees over room temperature [41], suggesting that this system is a far more sensitive substrate to examine energy deposition into multiply charged proteins via ion–ion reactions than are the covalently bound systems studied to date.

Experimental

Horse skeletal muscle holomyoglobin was obtained from Sigma Chemical Company (St. Louis, MO). Perfluoro-1, 3-dimethylcyclohexane (PDCH) was purchased from Aldrich (Milwaukee, WI). Solutions for electrospray were prepared by dissolving a sufficient quantity of the analyte in ultra-pure water from a Milli-RO/Milli-Q UVIS system (Millipore Corp., Bedford, MA) to provide a concentration of ~ 6 μM. To prevent denaturation of the holomyoglobin, no other solvents or acids were added to the solution. Electrospray signal was maximized by using a "nanospray" device fashioned in-house from a prepulled (10-μm-i.d. tip) borosilicate glass micropipette (World Precision Instruments, Sarasota, FL) with a luer fitting. Analyte solution was delivered to the pipette through our conventional stainless steel electrospray capillary at a rate of 0.1–0.2 μL min^{-1} via a syringe pump. The electrospray capillary was anchored within the micropipette with a standard high-performance liquid chromatography (HPLC) luer fitting and union, which also were used to make high voltage contact to the solution.

All experiments were carried out with this homemade electrospray source coupled with a Finnigan-MAT (San Jose, CA) ion trap mass spectrometer modified for injection of ions formed external to the ion trap through an endcap electrode. Details of the electrospray–ion trap interface have been described elsewhere [25]. Further modifications have been made to this apparatus to allow anions to be injected through a 3-mm-diameter hole drilled through the ring electrode. Details of these modifications and others made to facilitate analysis of high mass-to-charge ratio ions will be reported elsewhere [42]. A brief description of the hardware changes is given here.

An atmospheric sampling glow discharge ion source has been mounted on a side port of a 6-in.^{3} vacuum chamber used to support the ion trap assembly. The ion trap is situated such that there is a line of sight from the exit aperture of the glow discharge ion source to the 3-mm hole in the ring electrode. A lens stack is mounted off of the glow discharge ion source to facilitate ion transport to the ring electrode. The discharge is pulsed under software control via a high voltage solid state pulser (Directed Energy Inc., Fort Collins, CO, model GRX-1.5K-E). The output of the pulser is connected to the anode of the glow discharge source. The pulser acts as a fast switch that alternates between a voltage sufficient to strike a discharge (−400 V, as normally provided by an ORTEC, Oak Ridge, TN, model 556 power supply) and ground. This arrangement allows for independent control of cation accumulation from the electrospray and anion accumulation from the glow discharge. For all experiments, the mul-

tiply charged myoglobin ions were accumulated in the ion trap prior to PDCH anion accumulation [42].

Myoglobin cations were injected axially into the trap for periods ranging from 0.2 to 0.4 s. The radiofrequency (rf) sine-wave amplitude applied to the ring electrode during ion injection ranged from 700 to 1200 V zero-to-peak. In all cases, helium was admitted into the vacuum system to a total pressure of 1 mtorr with a background pressure in the instrument of 2×10^{-5} torr without the addition of helium. Anions were formed by sampling the head space vapors of PDCH into the glow discharge operated at 950 mtorr. For all ion–ion reactions described, anion accumulation periods ranged from 10 to 20 ms. The maximum mutual storage time for ion–ion reaction experiments was 105 ms.

Mass-to-charge ratio analysis was effected after the completion of all ion isolation and reaction periods by using resonance ejection to yield a mass-to-charge ratio range (for singly charged holomyoglobin) as high as 20,000 by using resonance ejection amplitudes of 2–3 V peak-to-peak. The spectra shown here were typically the result of an average of 10–20 individual scans.

Results and Discussion

The electrospray mass spectrum of horse skeletal muscle myoglobin dissolved in pure water (6 μM) is shown in Figure 1. Multiply charged ions corresponding to holomyoglobin and apomyoglobin are both apparent in the spectrum and the ionized heme group (not shown) was also present at m/z 617. It was noted that the relative abundances of the holo- and apomyoglobin ions (as well as that of the ionized heme group) were highly sensitive to interface conditions. As expected, higher voltage gradients in the interface gave rise to larger relative contributions from the apomyoglobin and heme ions. Interface conditions for this work were chosen to minimize fragmentation of the holomyoglobin ions while maintaining satisfactory transmission through the interface.

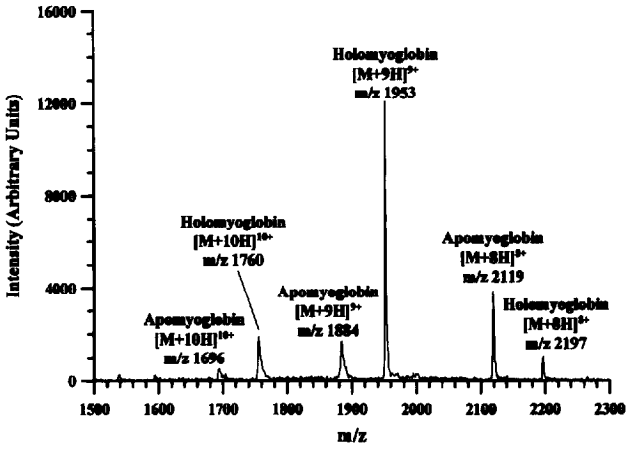

Figure 1. Electrospray mass spectrum of a 6-μM (100% water) solution of holomyoglobin. Interface conditions were optimized for transmission of the heme-containing holomyoglobin ions.

Figure 2 compares spectra acquired after isolation of the 9+ charge state of holomyoglobin without the subsequent addition of anions (Figure 2a) and with the subsequent addition of the $[M - F^{\cdot}]^-$ and $[M - CF_3^{\cdot}]^-$ anions derived from perfluoro-1,3-dimethylcyclohexane (PDCH) followed by a reaction period of 105 ms (Figure 2b). These anions thus far have been observed to react exclusively by proton transfer with multiply protonated molecules [15, 30, 34] and appear to do so with the holomyglobin ions as well. As noted previously [40], no evidence for loss of the heme group is apparent on the time frame of these experiments (tens to hundreds of milliseconds) following isolation of the holomyoglobin ions under normal ion trap storage conditions and in the presence of helium bath gas at 1 mtorr and at room temperature. Most noteworthy, no loss of heme is observed as a result of multiple ion–ion proton transfer reactions. For the 1+ ions (formed by eight consecutive ion–ion proton transfer reactions), fragmentation via loss of ionized or neutral heme associated with any of these steps would be reflected in the appearance of low charge state apomyoglobin ions. The lack of evidence for apomyoglobin ions in Figure 2b indicates that the exothermicity associated with ion–ion proton transfer from each of the holomyo-

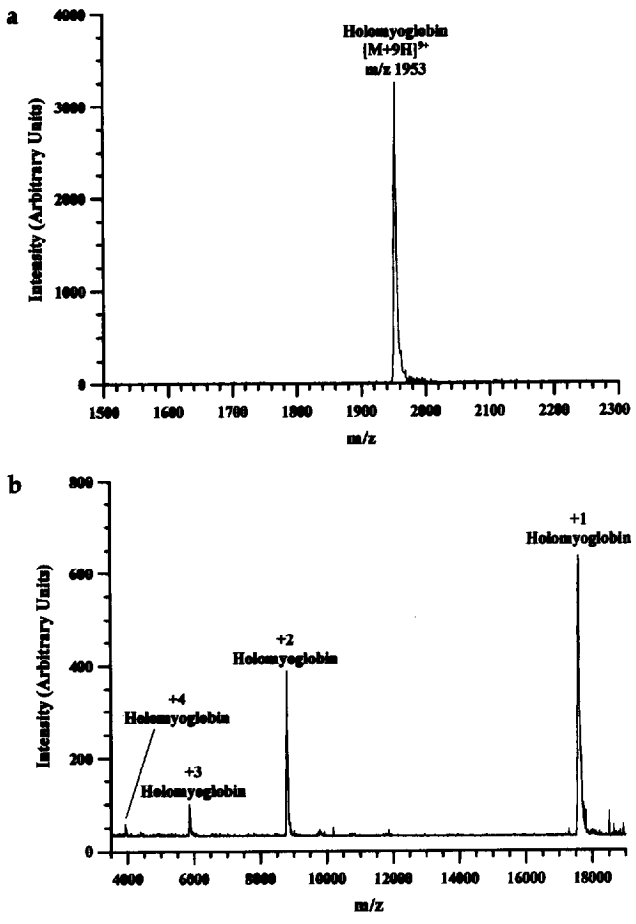

Figure 2. (a) Isolation of the 9+ charge state of holomyoglobin. (b) Reaction of the 9+ charge state of holomyoglobin with PDCH anions for approximately 110 ms.

globin charge states from 9+ to 2+ is insufficient to drive the loss of heme to an observable extent on the time frame of the ion trap experiment. It further suggests that local three dimensional structure that allows myoglobin to bind the heme group is present in all charge states from 9+ to 1+.

Factors that determine the extent to which fragmentation of a product of an ion–ion reaction is observed in the Paul trap include the reaction exothermicity, energy partitioning between translation and internal modes of the products, critical energies for dissociation, numbers of degrees of freedom of the product, observation time, and the cooling rates (both collisional and radiative). A recent study involving ion–ion recombination, a situation in which all of the reaction exothermicity is partitioned into internal energy of the condensation product, suggested that much of the excess internal energy initially present in the collision complex is removed via collisions with the helium bath gas present in the Paul trap before the complex can dissociate (at least for high mass complexes that behave statistically) [43]. Specifically, for a collision complex of the approximate size of bovine insulin A-chain, most of the internal energy associated with ion–ion recombination is removed via collisions with helium well within a millisecond. Although several of the quantities mentioned in the preceding test that affect the extent to which fragmentation of an ion–ion reaction product may occur (such as reaction exothermicity as a function of charge state) are not known for this system, several semiquantitative conclusions can be drawn from the data of Figure 2 by making a few reasonable assumptions, as subsequently described.

Provided the anion population is present in excess such that its number density can be considered to be constant, the data of Figure 2b result from a series of consecutive irreversible pseudo-first-order reactions. The time dependent abundance of the initial reactant, MH_n^{n+}, where $n = 9$ in the case of Figure 2, is simply

$$[MH_n^{n+}]_t = [MH_n^{n+}]_0 \exp^{(-Nk(n)t)} \quad (1)$$

where N is the anion number density, $k(n)$ is the ion–ion rate constant for the nth charge state cation, and t is reaction time. Kinetic equations can be written for each charge state incorporating the rate constant, $k(n)$, for each charge state. However, the expressions can be simplified in the case of ion–ion reactions by assuming that the rate constants are related by the square of the charge state [30]. That is, the ion–ion rate constant for the nth charge state is n^2 greater than that for the 1+ charge state. Such a relationship has been demonstrated for ion–ion proton transfer of the various charge states derived from bovine ubiquitin in reactions with the same anions derived from PDCH that were used to obtain the data of Figure 2. This observation is expected to be general due to the fact that the long range attraction governing ion–ion reactions is dominated by the Coulomb potential and the high exothermicity associated with ion–ion reactions tends to make them unit efficient. Making this assumption, therefore, the time dependence of the initial reactant ion can be rewritten as

$$[MH_n^{n+}]_t = [MH_n^{n+}]_0 \exp(-Nn^2kt) \quad (2)$$

where k is the ion–ion rate constant for the singly charged cation. The time dependence for the $MH_{(n-1)}^{(n-1)+}$ ion is given as

$$\left[MH_{(n-1)}^{(n-1)+}\right]_t = [MH_n^{n+}]_0 n^2 \left[\frac{\exp(-Nn^2kt)}{((n-1)^2 - n^2)} + \frac{\exp(-N(n-1)^2kt)}{(n^2 - (n-1)^2)}\right] \quad (3)$$

The time dependence for the $MH_{(n-2)}^{(n-2)+}$ ions is

$$\left[MH_{(n-2)}^{(n-2)+}\right]_t = [MH_n^{n+}]_0 n^2(n-1)^2 \times \left[\frac{\exp(-Nn^2kt)}{([n-1]^2 - n^2)([n-2]^2 - n^2)} + \frac{\exp(-N(n-1)^2kt)}{(n^2 - [n-1]^2)([n-2]^2 - [n-1]^2)} + \frac{\exp(-N(n-2)^2kt)}{(n^2 - [n-2]^2)([n-1]^2 - [n-2]^2)}\right] \quad (4)$$

Expressions for the time dependencies for the remainder of the charge states follow this pattern such that the time dependence for the singly charged ion, MH^+, is given as

$$[MH^+]_t = \{[MH_n^{n+}]_0 n^2(n-1)^2(n-2)^2 \cdots (n-7)^2\} \times \left[\frac{\exp(-Nn^2kt)}{([n-1]^2 - n^2)([n-2]^2 - n^2)([n-3]^2 - n^2) \cdots ([n-8]^2 - n^2)} + \frac{\exp(-N(n-1)^2kt)}{(n^2 - [n-2]^2)([n-2]^2 - [n-1]^2)([n-3]^2 - [n-1]^2) \cdots ([n-8]^2 - [n-1]^2)} + \frac{\exp(-N(n-8)^2kt)}{(n^2 - [n-8]^2)([n-1]^2 - [n-8]^2)([n-2]^2 - [n-8]^2) \cdots ([n-7]^2 - [n-8]^2)}\right] \quad (5)$$

The time dependence for the abundance of the completely neutralized protein is simply given as

$$[M]_t = [MH_n^{n+}]_0 - \left([MH_n^{n+}]_t + \left[MH_{(n-1)}^{(n-1)+}\right]_t + \left[MH_{(n-2)}^{(n-2)+}\right]_t + \cdots + [MH^+]_t\right) \quad (6)$$

Making the assumption that the ion–ion collision rate constant is determined by the Coulomb attraction between opposite charges, the ion–ion collision rate constant, k_c, is given by [30]

$$k_c = v\left(\frac{\pi}{2}\right)\left[\frac{Z_1 Z_2 e^2}{\mu v^2}\right]^2 \quad (7)$$

where v is the relative velocity, Z_1 is the charge of the cation, Z_2 is the charge of the anion, and μ is the reduced mass of the collision pair. For the case of singly protonated holomyoglobin, this rate constant, assuming thermal energy reactants, is roughly 8.24×10^{-8} cm^3 ion^{-1} s^{-1}. Figure 3 shows a calculated set of relative abundance curves for the various cationic ion–ion reaction products arising from MH_9^{9+} as a function of reaction time assuming that the anion number density is constant and a value of k of 8.24×10^{-8} cm^3 ion^{-1} s^{-1}. The curves can be fitted to the data of Figure 2b via the anion number density. The curves of Figure 3 were generated by using an anion number density of 6.4×10^7 cm^{-3}, which gives a good fit to the data of Figure 2b assuming a reaction period of 110 ms. (A 10-ms anion accumulation period was used in the experiment that gave rise to Figure 2b during which time the holomyoglobin ions were already present in the ion trap. This situation introduces uncertainty into the length of the reaction period because the anion number density changes very rapidly during this time. This error is relatively small, however, given that the programmed mutual storage time was 105 ms. A vertical line is drawn at a reaction time of 110 ms in Figure 3 to indicate the point in the abundance versus reaction time curves of relevance to the data of Figure 2b.) This anion number density is quite reasonable given that the maximum density for anions of m/z 331–381 under these conditions, by using the pseudopotential well-depth approximation [44], is roughly 2.7×10^8 cm^{-3}. [For comparison, the calculated maximum densities for the protein cations under these conditions is 5.1×10^7 cm^{-3} (9+ charge state) to 5.7×106 cm^{-3} (1+ charge state). The observed rate of reaction, however, is independent of cation number density provided the anions are present in great excess, as in these studies, such that pseudo-first-order kinetics prevail.]

It is the product of the rate constant and anion number density, that is, the proton transfer rate of singly charged holomyoglobin with the PDCH anions, that is used to fit the curves of Figure 3 with the data of Figure 2b. The fit is particularly good for the relative

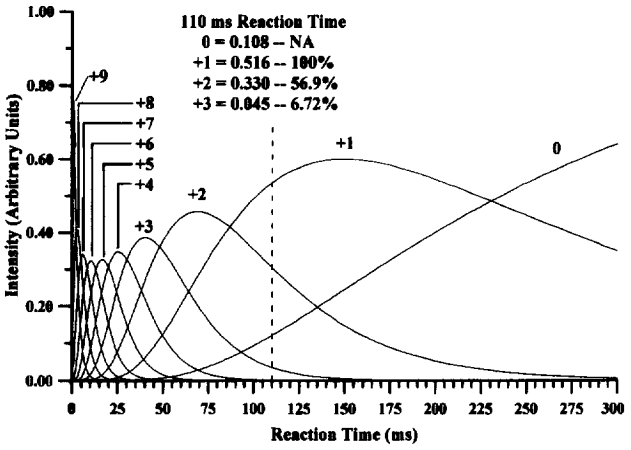

Figure 3. Relative cation abundances resulting from the reactions of the 9+ charge state of holomyoglobin and its consecutive reaction products with anions of PDCH ($k = 8.24 \times 10^{-8}$ cm^3 ion^{-1} s^{-1}; anion number density = 6.4×10^7 cm^{-3}) generated by the kinetic equations (i.e., eqs 2–5) described in the text. The calculated relative abundances of the 1+, 2+ and 3+ charge states for a reaction time of 110 ms (100, 56.9, 6.72) agree well with those obtained experimentally from Figure 2b (100, 61.5, 10.7), respectively.

abundances of the triply, doubly, and singly charged ions. The calculation does not predict the quadruply charged ion to be observed, but a small signal is apparent in the spectrum. Although this could indicate a shortcoming of the model used here to fit the data, the appearance of a small signal for the quadruply charged ion is more likely to result from the fact that the anion number density can vary by as much as a factor of 2 over the course of the averaging period. This variability introduces some dispersion in the shapes of the experimentally derived ion abundance curves as a function of reaction time. The fit of Figure 3 was obtained with an ion–ion proton transfer rate of 5.26 s^{-1} for the singly charged holomyoglobin ion. This rate, and the assumptions that the anion number density is constant and that rates scale as n^2, can be used to determine the approximate average time between successive proton transfer reactions. For example, at a rate of 5.26 s^{-1}, singly charged holomyoglobin ions on average undergo a collision with an anion every 190 ms. At the other extreme, the MH_9^{9+} ion reacts at a rate of 426 s^{-1}, yielding an average time between ion–ion collisions of 2.3 ms. The MH_8^{8+} ions formed from proton transfer from the MH_9^{9+} ions survive for roughly 3.0 ms before the next ion–ion collision. Figure 4 shows a plot of the average time between ion–ion collisions as a function of cation charge state. Assuming an average collision cross section for a holomyoglobin ion of roughly 1600 Å^2 [45], the ion–helium bath gas collision rate is roughly 7×10^5 s^{-1}. There are, therefore, several thousand thermalizing ion–helium collisions between proton transfer reactions for the most highly charged ions associated with the experiment leading to Figure 2 (see subsequent text). Increasingly longer average storage

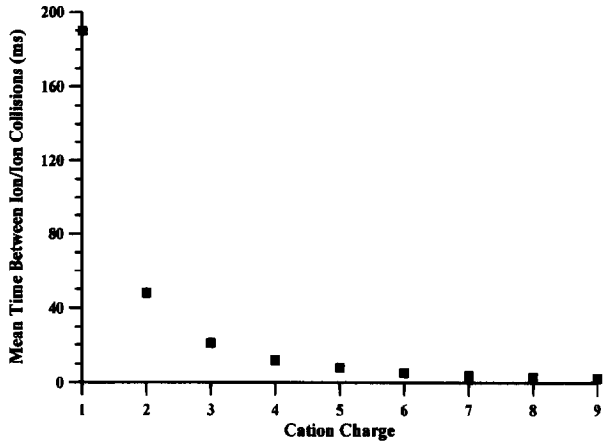

Figure 4. Mean time between ion–ion collisions as a function of charge state.

times between ion–ion collisions are in effect as the cation charge state decreases such that there are, on average, 36,000 ion–helium collisions after formation of the doubly charged ion and prior to the subsequent ion–ion collision.

Given the fact that proton transfer reaction exothermicity is governed by the difference between the proton affinity of the anion and the proton affinity of the product cation [30] and that cation proton affinities tend to decrease with charge [31], ion–ion proton transfer exothermicities are expected to be highest for the most highly charged ions. It is these ions that also undergo the highest rates of ion–ion collisions. It therefore follows that if no fragmentation results in the first few ion–ion collisions, it is unlikely that fragmentation will occur from the lower charge state ions unless some structural change associated with the loss of charge reduces the lowest critical energy for fragmentation. In the case of holomyoglobin, the binding of the heme group in the gas phase is sufficiently strong for each charge state to survive storage in the presence of room temperature helium for at least tens of milliseconds and possibly much longer.

The lack of fragmentation observed for the holomyoglobin ions, despite undergoing eight successive reactions that are exothermic by 4–7 eV each, is not surprising in the ion trap environment provided the lowest critical energy for decomposition is roughly 0.6 eV or greater for all charge states (where ions behave statistically). The latter proviso may not be strictly applicable in that all of the reaction exothermicity partitioned into the internal modes of the cation need not be completely randomized on a time scale faster than a typical dissociation rate for a relatively small ion. Rather, it suffices that the energy initially deposited at the reaction site dissipates quickly enough to avoid rapid dissociation in the general vicinity of the reaction site. Given the relatively high myoglobin ion–helium collision rate in the ion trap environment of roughly 700 m s^{-1}, dissociation rates should probably be greater than 10^4 s^{-1} to avoid significant removal of excess internal energy via collisions with the room temperature bath gas. Figure 5 shows a plot of the expected average number of ion–helium collisions per ion–ion collision as a function of charge state, as determined by the ion–helium collision rate divided by the ion–ion collision rate for each charge state. In this case the collision rate is assumed to be relatively constant as a function of charge state. Even for the highest myoglobin charge states, there are several thousand ion–helium collisions between ion–ion collisions. The accumulation of internal energy by successive ion–ion proton transfer reactions is therefore largely prevented by ion–helium collisions between each reaction. The previously mentioned critical energy cutoff of 0.6 eV is approximate and is based on the Rice–Ramsperger–Kassel–Marcus (RRKM) calculations of Griffin and McAdoo [46] for polypeptides of various sizes. The RRKM dissociation rate becomes increasingly sensitive to critical energy as the size of the polypeptide increases. For a polypeptide of the size of myoglobin, based on the assumptions used by Griffin and McAdoo in their RRKM calculations, a critical energy of 0.6 eV yields a dissociation rate of roughly 10^5 s^{-1} for a 298-K ion that is activated by a single 193-nm photon. Based on these numbers, a critical energy for heme loss significantly less than about 0.6 eV might have been expected to result in the observation of some loss of heme during the course of the ion–ion proton transfer experiment, depending upon the fraction of reaction exothermicity partitioned into the cation. Although the critical energy for heme loss from gas-phase holomyoglobin cations has not been reported, the Arrhenius activation energy in solution has been reported to be 1.1 ± 0.07 eV [47]. A critical energy of this magnitude for loss of heme from gas-phase holomyoglobin ions would make fragmentation under the ion–ion reaction conditions used here highly unlikely.

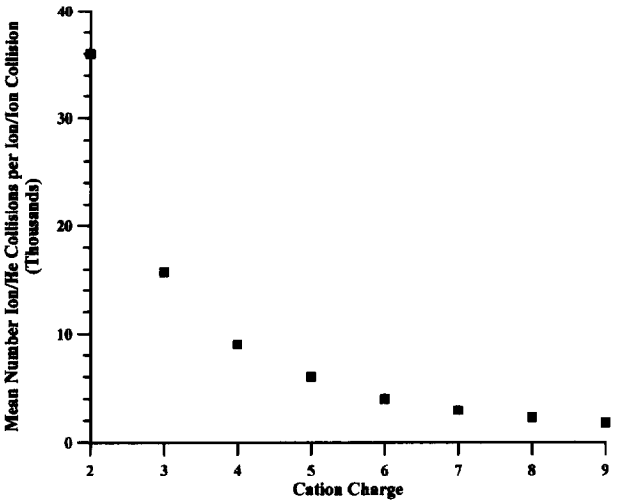

Figure 5. Mean number of ion–helium collisions per ion–ion collision as a function of charge state. The ion–helium collision rate is assumed to be independent of charge state.

Having established that gas-phase ion–ion proton transfer reactions involving holomyoglobin ions produce no measurable yields of apomyoglobin ions, it is possible to subject both holomyoglobin ions and apomyoglobin ions simultaneously to identical reaction conditions to compare the relative rates of reaction for the two species. Figure 6 shows the results of such an experiment in which all of the ions accumulated from the electrospray source, under conditions that yielded very similar numbers of apo- and holomyoglobin ions, were subjected to ion–ion proton transfer reactions for roughly 70 ms. After this reaction period, significant numbers of ions were observed in each of the charge states from 1 + to 4 +. Within experimental error, there are equal numbers of each ion type for every charge state in Figure 6. This can result only if the rates of reaction for each ion type are equal or very nearly so. The data indicate that these experiments could not distinguish a difference in the ion–ion proton transfer rates for holomyoglobin ions and apomyoglobin ions. For a given charge state, the only expected difference in ion–ion collision rate, based on eq 7, arises from the effect of the difference in mass of apomyoglobin and apomyoglobin on the reduced mass and relative velocity of the collision pair. This effect amounts to an expected rate difference of well under 1%. Although it cannot be concluded from these results that apomyoglobin and holomyoglobin ions of the same charge state both react at the expected collision rate (that is, with unit efficiency), because we have no independent measure of the anion number density, it can be concluded that they react with equal efficiency, within the precision of these measurements.

Recent measurements of ion kinetic energy losses associated with collisions of gaseous apomyoglobin and holomyoglobin ions with argon [39] have shown that, under some interface and solution conditions, holomyoglobin ions are more compact than apomyoglobin ions. However, it also has been shown that, for example, interface conditions can be found in which the collision cross sections are similar [39]. In the absence of such collision cross section measurements for the solution, interface, ion capture, and ion storage conditions used here, we cannot draw firm conclusions regarding the relative sizes of the two ion types with respect to collisions with neutrals. However, these measurements show that, within experimental error, the cross sections with respect to collisions with oppositely charged ions are the same. In the case of singly protonated holomyoglobin ions in collisions with the anions derived from PDCH, the calculated cross section, as determined by dividing the predicted rate constant by the relative velocity of the collision pair, is 59,000 Å^2. Although other such comparisons that might indicate a sensitivity of the ion–ion reaction rate to bio-ion structure are necessary to draw firm conclusions regarding the value of ion–ion reactions as a structural probe, these results support previous observations [30] that suggest that ion–ion proton transfer reactions involving bio-ions are not particularly sensitive to differences in high order structure. The high exothermicity of the reaction and the dominance of the Coulomb attraction at long range in determining the collision rate constant lead to the expectation that the reaction kinetics are dominated by the factors in eq 7. On the one hand, this implies that ion–ion proton transfer reactions are not useful structural probes; on the other hand, it implies that the rates of ion–ion reactions can be readily predicted, which makes ion–ion proton transfer reactions highly reliable means for manipulating bio-ion charge state.

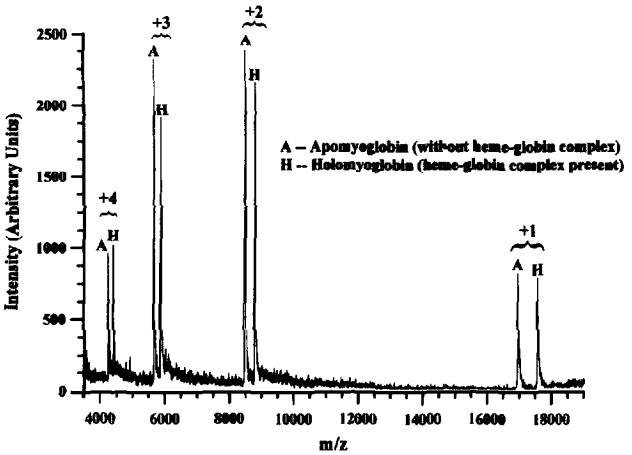

Figure 6. Spectrum of cationic products of apomyoglobin and holomyoglobin cations following proton transfer reactions with PDCH anions for approximately 70 ms.

Conclusions

Multiply protonated holomyoglobin can be deprotonated in a quadrupole ion trap operated with helium bath gas at 1 mtorr by anions derived from PDCH without measurable loss of the noncovalently bound heme group. Given that the ion lifetime is long relative to the ion–helium collision rate, fragmentation is not expected to occur. Furthermore, the high ion–helium collision rate relative to the ion–ion collision rate prevents the accumulation of internal energy via successive ion–ion reactions. The many degrees of freedom associated with high mass bio-ions makes even relatively weakly bound species, including at least some noncovalently bound specific bio-ion complexes, stable under ion–ion proton transfer reaction conditions in the ion trap. This result is significant in that it suggests that ion–ion proton transfer reactions can be used to manipulate the charge of noncovalently bound complexes without inducing fragmentation, provided charge itself is not an important criterion for binding. Holomyoglobin and apomyoglobin ions of the same charge state undergo ion–ion proton transfer reactions at indistinguishable rates. This observation lends support to the expectation that ion–ion proton transfer reactions are not sensitive to ion structure, which is a

positive characteristic for the use of ion–ion reactions as a tool for the manipulation of bio-ion charge.

Acknowledgments

J.L.S. acknowledges support through an appointment to the Oak Ridge National Laboratory Postdoctoral Research Associates Program administered jointly by the Oak Ridge Institute for Science and Education and Oak Ridge National Laboratory. This work was supported by the National Institutes of Health under grant no. R01GM45372. Oak Ridge National Laboratory is managed for the U.S. Department of Energy under contract no. DE-AC05-96OR22464 by Lockheed Martin Energy Research Corporation.

References

1. Fenn, J. B.; Mann, M.; Meng, C. K.; Wong, S. F.; Whitehouse, C. M. *Science* **1989**, *246*, 64.
2. Fenn, J. B.; Mann, M.; Meng, M. K.; Wong, S. F.; Whitehouse, C. M. *Mass Spectrom. Rev.* **1990**, *9*, 37.
3. Smith, R. D.; Loo, J. A.; Edmonds, C. G.; Barinaga, C. J.; Udseth, H. R. *Anal. Chem.* **1990**, *62*, 882.
4. Smith, R. D.; Loo, J. A.; Ogorzalek Loo, R. R.; Busman, M.; Udseth, H. R. *Mass Spectrom. Rev.* **1991**, *10*, 359.
5. Smith, R. D.; Loo, J. A.; Ogorzalek Loo, R. R.; Busman, M.; Udseth, H. R. *Mass Spectrom. Rev.* **1992**, *11*, 434.
6. Karas, M.; Hillenkamp, F. *Anal. Chem.* **1988**, *60*, 2299.
7. Overberg, A.; Karas, M.; Hillenkamp, F. *Rapid Commun. Mass Spectrom.* **1991**, *5*, 128.
8. Nordhoff, E.; Ingedoh, A.; Cramer, R.; Overberg, A.; Stahl, B.; Karas, M.; Hillenkamp, F.; Crain, P. F. *Rapid Commun. Mass Spectrom.* **1992**, *6*, 771.
9. Mahoney, J. F.; Perel, J.; Ruatta, S. A.; Martino, P. A.; Husain, S.; Lee, T. D. *Rapid Commun. Mass Spectrom.* **1991**, *5*, 441.
10. Mahoney, J. F.; Perel, J.; Lee, T. D.; Martino, P. A.; Williams, P. J. *Am. Soc. Mass Spectrom.* **1992**, *3*, 311.
11. McLuckey, S. A.; Glish, G. L.; Van Berkel, G. J. *Anal. Chem.*, **1991**, *63*, 1971.
12. Hunter, A. P.; Severs, J. C.; Harris, F. M.; Games, D. E. *Rapid Commun. Mass Spectrom.* **1994**, *8*, 417.
13. Herron, W. J.; Goeringer, D. E.; McLuckey, S. A. *Anal. Chem.* **1996**, *68*, 257.
14. McLuckey, S. A.; Goeringer, D. E. *Anal. Chem.* **1995**, *67*, 2493.
15. Stephenson, J. L., Jr.; McLuckey, S. A. *Anal. Chem.*, **1996**, *68*, 4026.
16. Smith, R. D.; Cheng, X.; Bruce, J. E.; Hofstadler, S. A.; Anderson, G. A. *Nature* **1994**, *369*, 137.
17. McLuckey, S. A.; Van Berkel, G. J.; Glish, G. L. *J. Am. Chem. Soc.* **1990**, *112*, 5668.
18. Ogorzalek-Loo, R. R.; Loo, J. A.; Udseth, H. R.; Fulton, J. L.; Smith, R. D. *Rapid Commun. Mass Spectrom.* **1992**, *6*, 159.
19. Winger, B. E.; Light-Wahl, K. J.; Smith, R. D. *J. Am. Soc. Mass Spectrom.* **1992**, *3*, 624.
20. Ikonomou, M. G.; Kebarle, P. *Int. J. Mass Spectrom. Ion Processes* **1992**, *117*, 283.
21. Cassady, C. J.; Wronka, J.; Kruppa, G. H.; Laukien, F. H. *Rapid Commun. Mass Spectrom.* **1994**, *8*, 394.
22. Ogorzalek Loo, R. R.; Smith, R. D. *J. Am. Soc. Mass Spectrom.* **1994**, *5*, 207.
23. Schnier, P. D.; Gross, D. S.; Williams, E. R. *J. Am. Chem. Soc.* **1995**, *117*, 6747.
24. Cassady, C. J.; Carr, S. R. *J. Mass Spectrom.* **1996**, *31*, 247.
25. McLuckey, S. A.; Van Berkel, G. J.; Glish, G. L.; Schwartz, J. C. In *Modern Mass Spectrometry: Practical Aspects of Ion Trap Mass Spectrometry*, Vol. 2; March, R. E., Todd, J. F. J., Eds., CRC Press: Boca Raton, 1995; Chap. 3, p 89.
26. Gross, D. S.; Rodriguez-Cruz, S. E.; Williams, E. R. *J. Phys. Chem.* **1995**, *99*, 4034.
27. Schnier, P. D.; Gross, D. S.; Williams, E. R. *J. Am. Soc. Mass Spectrom.* **1995**, *6*, 1086.
28. Gross, D. S.; Williams, E. R. *J. Am. Chem. Soc.* **1995**, *117*, 883.
29. Camara, E.; Green, M. K.; Penn, S. G.; Lebrilla, C. B. *J. Am. Chem. Soc.* **1996**, *118*, 8751.
30. Stephenson, J. L., Jr.; McLuckey, S. A. *J. Am. Chem. Soc.* **1996**, *118*, 7390.
31. Kaltashov, I. A.; Fenselau, C. *Rapid Commun. Mass Spectrom.* **1996**, *10*, 857.
32. Herron, W. J.; Goeringer, D. E.; McLuckey, S. A. *J. Am. Chem. Soc.* **1995**, *117*, 11555.
33. McLuckey, S. A.; Stephenson, J. L., Jr.; O'Hair, R. A. J. *J. Am. Soc. Mass Spectrom.* **1997**, *8*, 148.
34. Stephenson, J. L., Jr.,; McLuckey, S. A. *J. Am. Chem. Soc.* **1997**, *119* 1688.
35. Katta, V.; Chait, B. T. *J. Am. Chem. Soc.* **1991**, *113*, 8534.
36. Li, Y. T.; Hsieh, Y. L.; Henion, J. D.; Ganem, B. *J. Am. Soc. Mass Spectrom.* **1993**, *4*, 631.
37. Feng, R.; Konishi, Y. *J. Am. Soc. Mass Spectrom.* **1993**, *4*, 638.
38. Loo, J. A.; Giordani, A. B.; Muenster, H. *Rapid Commun. Mass Spectrom.* **1993**, *7*, 186.
39. Collings, B. A.; Douglas, D. J. *J. Am. Chem. Soc.* **1996**, *118*, 4488.
40. McLuckey, S. A.; Ramsey, R. S. *J. Am. Soc. Mass Spectrom.* **1994**, *5*, 324.
41. Herron, W. J.; Goeringer, D. E.; McLuckey, S. A. *Proceedings of the 42nd ASMS Conference on Mass Spectrometry and Allied Topics*; May 29–June 3, 1994; p. 213.
42. Stephenson, J. L., Jr.; McLuckey, S. A. *Int. J. Mass Spectrom. Ion Processes* in press.
43. McLuckey, S. A.; Herron, W. J.; Stephenson, J. L., Jr.; Goeringer, D. E. *J. Mass Spectrom.* **1996**, *31*, 1093.
44. March, R. E.; Hughes, R. J. *Quadrupole Storage Mass Spectrometry*, Wiley: New York, 1989; p 201.
45. Covey, T. R.; Douglas, D. J. *J. Am. Soc. Mass Spectrom.* **1993**, *4*, 616.
46. Griffin, L. L.; McAdoo, D. J. *J. Am. Soc. Mass Spectrom.* **1993**, *4*, 11.
47. Hunter, C. L.; Mauk, A. G.; Douglas, D. J., unpublished.